

PRODUCTION OF PROFILE AND THREE DIMENSIONAL SURFACE MAPS OF A MICRO PORTION ALONG THE NIGERIAN COAST, LAGOS STATE, NIGERIA

Oladosu S. O.^{1*}, Alademomi A. S.² and Ayodele E. G.²

¹Department of Geomatics, Faculty of Environmental Sciences, University of Benin, PMB 1154, Edo State, Nigeria.

²Department of Surveying and Geoinformatics, Faculty of Engineering, University of Lagos, P.M.B. 12003, Akoka, Lagos State, Nigeria.

*Corresponding Author's Email: olushola.oladosu@uniben.edu

(Received: 15th September, 2022; Accepted: 22nd December, 2022)

ABSTRACT

In this study, shoreline profile and three-dimensional surface map were created from an integrated topographic and bathymetric survey dataset obtained using global navigation satellite system operating in real-time kinematic (GNSS RTK) mode, a cutting-edge field measurement technique that has revolutionised and further reduced the burden of lengthy data collection times associated with traditional methods. After appropriate interpolation, the three-dimensional map produced shows how the transition from the land-water interface blended. The topographic elevation was 1.7 m, and the highest point measured from it was 8 m, while the bathymetric elevation was 0.5 m, and the highest sounding depth was -9 m. The computed uncertainties were $0.5 \text{ m} \pm 0.515$, and $5 \text{ m} + (-0.47)$ for the vertical and horizontal, respectively. The beachhead elevation ranges from +3 m to +6 m, and the cross-section of the beach has a uniform slope from the zero mark of the site datum over a horizontal distance of 230 m to an elevation of -7 m seaward. Subsequently, the bed topography rises slightly to describe an underwater ridge with a bump ranging between 1 m and 4 m in height. The profile then levels off at a very gentle gradient of between -8 m and -9 m in elevation. The formation of the underwater dune feature lies just at the front of the groyne heads. Its formation might have been influenced by the groynes. However, in the middle part of the profile map, the feature was not well pronounced. In conclusion, the information provided in this paper can assist in safe navigation and provides data for various engineering designs aimed at solving an environmental problem, such as the construction of shore protection for addressing coastal erosion in the study area.

Keywords: Beach, Coast, Depth, GNSS RTK, Profile, Tide.

INTRODUCTION

The Nigerian coastal zone stretches for 853 km with an Exclusive Economic Zone (EEZ) of 210,900 km² (Zabbey *et al.*, 2019). This region attracts commercial activities associated with agriculture, oil and gas exploration and exploitation, fishing, mining, and shipping (Croitoru *et al.*, 2020). It also plays a significant role in the sustainability of international trade affairs and the water transportation system. Of particular interest is Lagos State because it makes up 25% of the nation's economic strength and has 164 km of coastline, with 40% of the state's residents living along the coast (Croitoru *et al.*, 2020). Apart from Lagos State, the remaining eight states in Nigeria are (Akwa-Ibom, Bayelsa, Cross River, Delta, Edo, Ogun, Ondo, and Rivers), which together make up the coastal region.

The interactions of the land-sea interface in the coastal area are complex to study, being heavily influenced by both natural processes and artificial or human influences (Kannan *et al.*, 2013). Among the noticeable ones is the beach profile dynamics

(Emery, 1961; Lewicka *et al.*, 2021). Seasonal accretion and erosion are usually prevalent at the intertidal (surf zone). Detection of changes in bed elevation requires some form of survey measurement that may be carried out once or repeatedly as occasion and purpose demand (Lewicka *et al.*, 2021). The information provided through profile measurement undertaken by nearshore and 3D mapping is of great importance to coastal/marine engineers and hydrographers (USGS, 2017; Genchi *et al.*, 2020). Those concerned with safe navigation, vessel safety, shore protection, structural monitoring, cross-shore, and long-shore sediment transport assessment relied on adequate shoreline data and information (Freeman *et al.*, 2003). Besides, appropriate shoreline description is required for beach nourishment and stability investigation, storm surge and sea-level-rise modeling, benthic and habitat mapping, coral reef-ecosystem mapping, seasonal shoreline change detection, and so on (Gable and Wanetick, 1984; Freeman *et al.*, 2003; USGS, 2017; Genchi *et al.*, 2020). The construction of shore protection or beach

nourishment has become one of the most commonly used methods to mitigate beach erosion (Cheng *et al.*, 2016). However, the construction of a structure such as a groyne affects the natural state of the undisturbed shoreline. Kraus (2005) opined that understanding the beach profile and its importance in planning for safe coastal management is one of the most studied features of coastal morphology.

The shape assumed by the beach profile determines how vulnerable the coast is to storms or flash floods (Kim *et al.*, 2014). Due to emerging improvements in methodology and technological advancements in survey instrumentation, researchers have conducted beach profile surveys for shore studies in different ways and capacities (Vriend and Koningsveld, 2012; Neshaei and Biria, 2013; van der Spek *et al.*, 2020). The conventional boat-sonic depth sounder, the hydrostatic pressure profiler, and the self-powered Coastal Research Amphibious Buggy (CRAB) are the three most common survey techniques used to measure nearshore profiles, according to Gable and Wanetick (1984). Improved methods applied to acquire data for monitoring changes in beach profiles are discussed in (Gable and Wanetick, 1984; Cheng *et al.*, 2016). These survey methods are the Total Station method, the GNSS-RTK method, the UAVs/Drones method, the LiDAR system technique, the Video Imaging system approach, the Photogrammetry principle, and the Remote Sensing method. Each of these methods has its own specific advantages and drawbacks. The purpose for which the survey is conducted, the cost implications, the project life cycle, the scope of the project, and so on will determine, to a greater or lesser extent, the resolution and the appropriateness of any chosen techniques. When available, time-series beach-profile and 3D data are good for describing the evolution of beach hydrodynamics, geodynamics, and metaphoric processes (Cheng *et al.*, 2016). It could allow for quantitative evaluation of beach nourishment or protection project design, performance and contribute meaningful success to coastal management (Emery, 1961; Anders and Byrnes, 1991; Crowell *et al.*, 1991; Kaliraj *et al.*, 2014; Kankara *et al.*, 2015; Cheng *et al.*, 2016; Badejo and Akintoye, 2017).

When processed, the geospatial dataset captured through the profile survey nearshore could provide invaluable information for describing the morphology and other key beach features such as the berm, sand bars, or dunes, as well as the characteristics of nearshore, submerged, and emerged topography. By comparing the latest data to past data, researchers can estimate the volume of sand lost due to (erosion) or the amount of sand gained by (accretion) over a specific time interval. The result assists the beach managers and coastal engineers in determining the best approach for beach nourishment, including the cost analysis for sand replacement or reclamation (Neshaei and Biria, 2013; Cheng *et al.*, 2016; Badejo and Akintoye, 2017).

Since no time-series or long-term data were collected in this work, a possible way to display the surf zone topography information is to show the profile and 3D characteristics along the common boundary of water and land. The limitation regarding this work, therefore, is that no morphological change or comparison can be made from a single observation campaign. However, this research aims to provide insight into the profile of the surf zone, x-ray possible impediments to smooth navigation, and generate the dataset needed for the design and construction of engineering structures like shore protection for the safety of the adjoining proposed Maiyegun estate.

MATERIALS AND METHODS

Description of the Study Area

The study area which covers (2.0 m x 400 m = 800 m²), or about 0.8 km² is located in Eti-Osa Local Government Area (LGA) of Lagos State. Lagos State contributes the largest stretch of the Nigeria coastal zone. The geographic description in easting and northing coordinates are: 3° 28' 00" E; 6° 26' 00" N and 3° 31' 00" E; 3° 24' 00" N in zone 31 N of the Universal Transverse Mercator (UTM). The survey extent covered from West to East of Groyne-8 through to Groyne-12 (bay-1 to bay-5) from longitude 3° 29' 48.16" E to 3° 30' 54.87" E, with a separating distance of about 2 km. Again, from the North through to the South, the survey extended from the +2.0 m Chart Datum contour to about 100 m beyond the heads of the groynes, for a distance of 400 m. The contouring of the

entire area was at depth interval of 0.5 m and the creation of sections was set at 50 m intervals along the length of the beach. Figure 1 shows the map of Lagos State and the location of the study area.

The methodology and the procedures followed are briefly summarised in the workflow diagram presented in Figure 2.

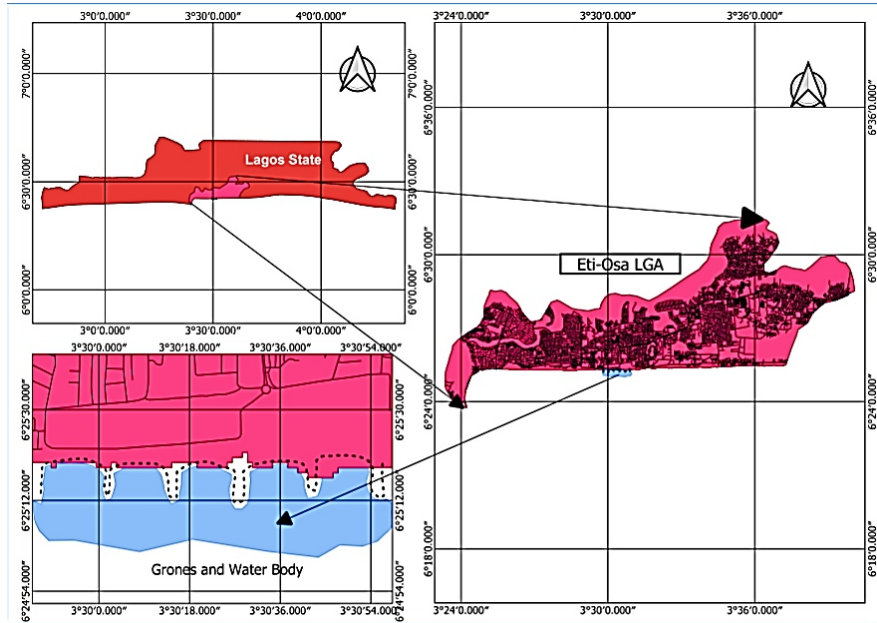


Figure 1: Map of Lagos State showing the location of the study area (after Oladosu *et al.*, 2022).

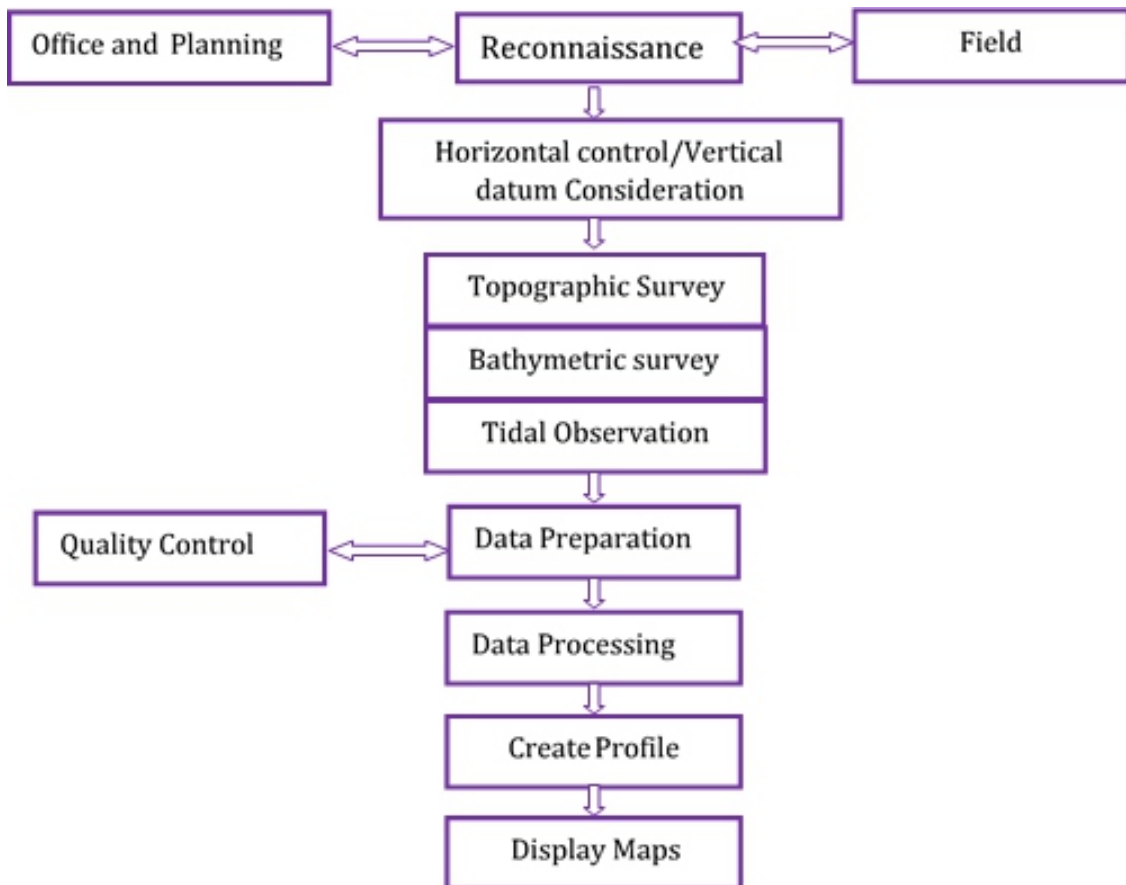


Figure 2: Conceptual workflow diagram of the study.

Topographic Survey Data Acquisition

Data acquisition for the topographic survey was carried out by setting the global navigation satellite system (GNSS) base receiver on the established vertical control (benchmark ME2). A preliminary reconnaissance survey provided the information that guided the creation of an AutoCAD file containing the coordinates of the extent of the survey, which was later loaded to the real-time kinematic (RTK) handheld controller for navigation and collection of the needed data for the required lines. Points on the beach were picked via RTK-GNSS strictly at low tide. A depth of (-1.5 m) was often achieved from the shore toward the sea. Plate 1 shows the location of the ME2 control station (left) and RTK base station (right) at a suitable point on the beach for ease of radio transmission in the study area.

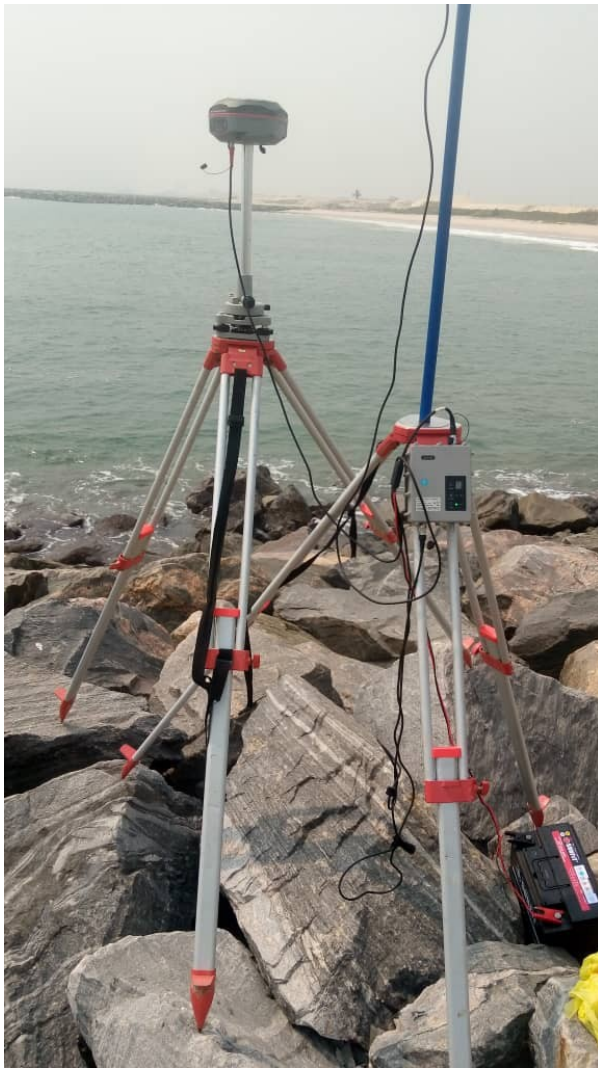


Plate 1: Positions of the bench mark and the RTK base station control point.

Bathymetric Survey Data Acquisition

Bathymetric survey data was collected using an echo sounder mounted on a hydrographic standard vessel measuring 7 m in length and 3 m in width and powered by 75 HP Yamaha engines. The transducer was mounted on the port side of the vessel, and the RTK-GNSS antenna was mounted in synergy vertically above it, resulting in zero offsets. To ensure that the echo sounder reading was accurate and to make any necessary corrections to the determined depths, a bar check was performed on a 5 m standard bar graduated at a 1 m interval. The draft of 0.3 m obtained was also supplied to the equipment before the final depths were accepted. The 36 predefined transect lines spaced at 50 m intervals already loaded into the Hypack software were traversed using the onscreen user guide provided by the software vendor.

The Kolida K5-UFO GNSS rover provided the corrected GNSS-derived latitude and longitude position to the Toshiba Laptop. For horizontal positioning, the antenna position was converted to Minna Clark's 1880 local datum. The Lagos Datum of 1955, reported by Badejo *et al.*, (2014), was used for the vertical positioning reference. The RTK antenna height is measured from the antenna reference point to the water level to provide continuous readings of the water level, while the echo-sounder measures the water level to the seabed. This configuration reduces vessel heave and enables the storage of 1-second tide readings in the software's hard disk for onshore processing. It also allows for the direct measurement of seabed elevation relative to the datum. The echo sounder provided the depth, while RTKGNSS provided the corresponding horizontal coordinates. To understand how the echo sounder uses acoustic pulse energy to determine depth, equation 1 (Ibrahim *et al.*, 2022) is typically applied. Figure 3 is a diagram that demonstrates this principle.

$$d = \frac{1}{2}vt - k + dr \quad (1)$$

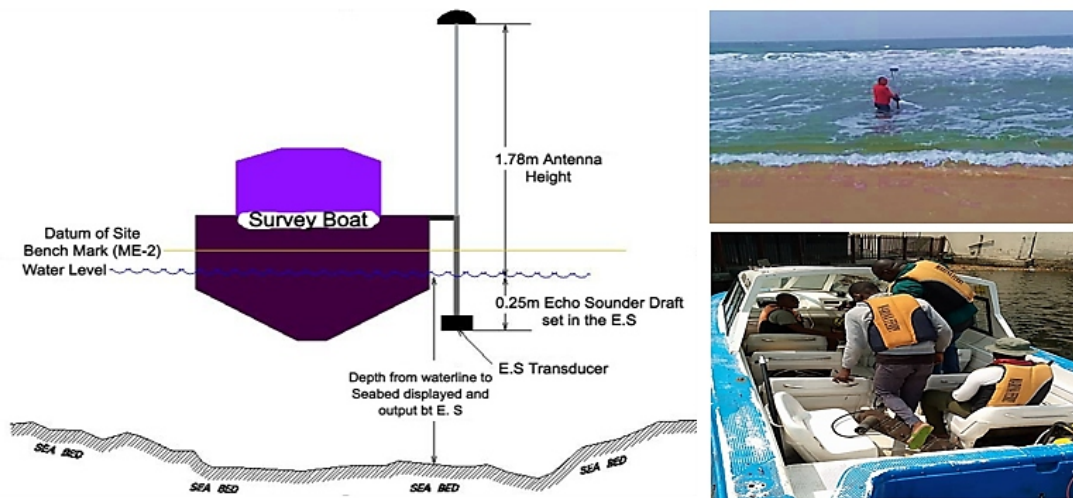


Figure 3: Schematic diagram of the procedure.

Tidal Observation and Water Level Monitoring

Me2 provided both horizontal and vertical control information since it was coordinated in 3D (X, Y, and Z). Its coordinates in UTM Zone 31 N are given as: (556624.604 m E: 710184.814 m N: 3.527 m). The TID-1 and the TID-2, are two additional benchmarks marked at the groyne and coordinated from (ME2) on a stable sand fill portion above flood level. Their 3D coordinate values are TID-1 (556665.415 m E: 709746.679 m N: 3.094 m) and TID-2 (556662.522 m E: 709711.657 m N: 3.338 m), respectively. The Tidemaster tide gauge was calibrated by mounting the RTK-GNSS rover on a buoy to read the water level to the ME2 benchmark at low ebb. The MSL was found to be 0.1 m below the zero of ME2, according to the information obtained from the tidal analysis table. This suggests that the level of ME2 above MSL is equivalent to 3.527 m plus 0.1 m, which when added together gives 3.627 m. The

Lagos Chart Datum (LCD) is equivalent to zero of ME2 minus 1.1 m ($1.5 \text{ m} - 0.4 \text{ m} = 1.1 \text{ m}$) or by using MSL minus 1.0 m ($1.1 \text{ m} - 0.1 \text{ m} = 1.1 \text{ m}$). The result of the on-site calibration of the Tidemaster tide gauge and the RTK-GNSS showed the means of both to be 1.451 m and -0.313 m, respectively. The TideMaster WL was therefore corrected as ($-0.326 \text{ m} - 1.456 \text{ m} = -1.782 \text{ m}$), or ($-0.313 \text{ m} - 1.451 \text{ m} = -1.764 \text{ m}$), which can be approximated to -1.8 m. Hence, we corrected the raw gauge readings by -1.8 m to bring their values to the height of ME2. The Nigerian Navy Dockyard Quay, with geographic coordinates (Latitude: 006-25-20.81 N; Longitude: 003-24-21.78 E), served as an independent check station against disturbing wave action since such characterisation is allowed in hydrography. Plate 2 shows the pictures and the Google Earth image of the locations. Figure 4 shows the charts of the calibration process for both methods considered.



Plate 2: Locations of TID1 and TID 2 and the Nigerian Navy dockyard tide Gauge.

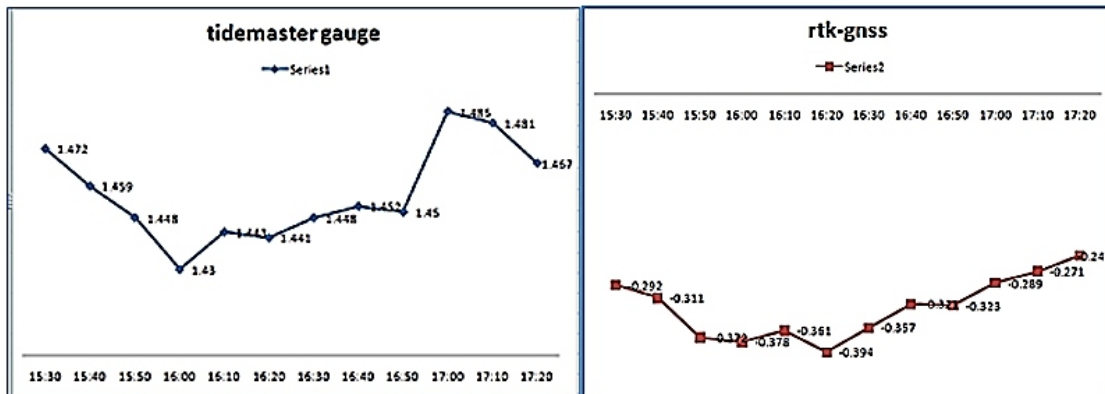


Figure 4: Charts of the calibration of Tidemaster and rtkGNSS buoy.

Inverse Distance Weighting Interpolation

IDW was used to predict an unsampled location spanning 20 m to 60 m for the bathymetric and topographic surveys to overlap. IDW is a deterministic estimation method that investigates the potential of obtained values at measured points to determine those at unmeasured points using a linear combination of nearest neighbour similarity characteristics (Wu and Hung, 2016). The predicted elevations using the IDW interpolation method embedded in Surfer software. This model is represented by equation 2.

$$x^* = \frac{w_1x_1 + w_2x_2 + w_3x_3 + \dots + w_nx_n}{w_1 + w_2 + w_3 \dots + w_n} \tag{2}$$

where, $w = \frac{1}{d_{ix}^p}$

Where x^* is unsampled location to be determined, w is the weight, and x are the locations whose value are known. The weight is the inverse of the distance of a point to the value of each known used for computation.

Bathymetric and Topographic Quality Control

As part of the quality control measures taken during the bathymetric survey, bar checks were

performed before and after the bathymetry to ensure the echo sounder recorded the accurate depth. For the topographic survey, a “double check approach” was used, in which elevation was transferred from the base station ME2 to a new station TID2. The TID2 surveys were conducted twice on two different days, and the results, with a millimeter of error, were consistent enough to make it serve as a tide monitoring station. The

final quality control check was the vertical and horizontal uncertainties. The International Hydrographic Organization (IHO, 2020) and the United States Geological Survey (USGS, 2017) provide information for calculating these uncertainties. For this work, Table 1 summarises the parameters for computation and the final results obtained after application.

Table 1: Horizontal and vertical uncertainties in obtained bathymetric data.

Uncertainty Order 1a	Parameter (a)	Parameter (b)	Parameter (d)	Product (b) x (d)	Formulae	Results
Total Vertical Uncertainty (TVU) 95% CL	0.5m	0.013	-9.4m	-0.1222m	$\pm\sqrt{a^2 + (b \times d)^2}$	± 0.515
Total Horizontal Uncertainty (THU) 95% CL	N/A	N/A	-9.4m	N/A	$5m + (5/100) * d$	$5m + (-0.47)$

Note: *N/A* -denotes not-applicable; (*a*): -signifies the portion of uncertainty that is invariant with dept; (*b*): - refers to a coefficient representing the portion of uncertainty that varies with the measured depth; (*d*): - is the maximum depth obtained seaward at observation period; (*b x d*): - represents the product of the portion of uncertainties that varies with the depth.

Preliminary Data Integration, Design and Plotting Process

The bathymetric and topographic data and the contour lines generated at the Maiyegun estate beachfront, including the location of wrecks on a

horizontal scale of 1:3000 and a vertical scale of 1:300 with elevation reference to ME2, are incorporated in the design of Figure 5. Also, the 36 transect lines were shown.

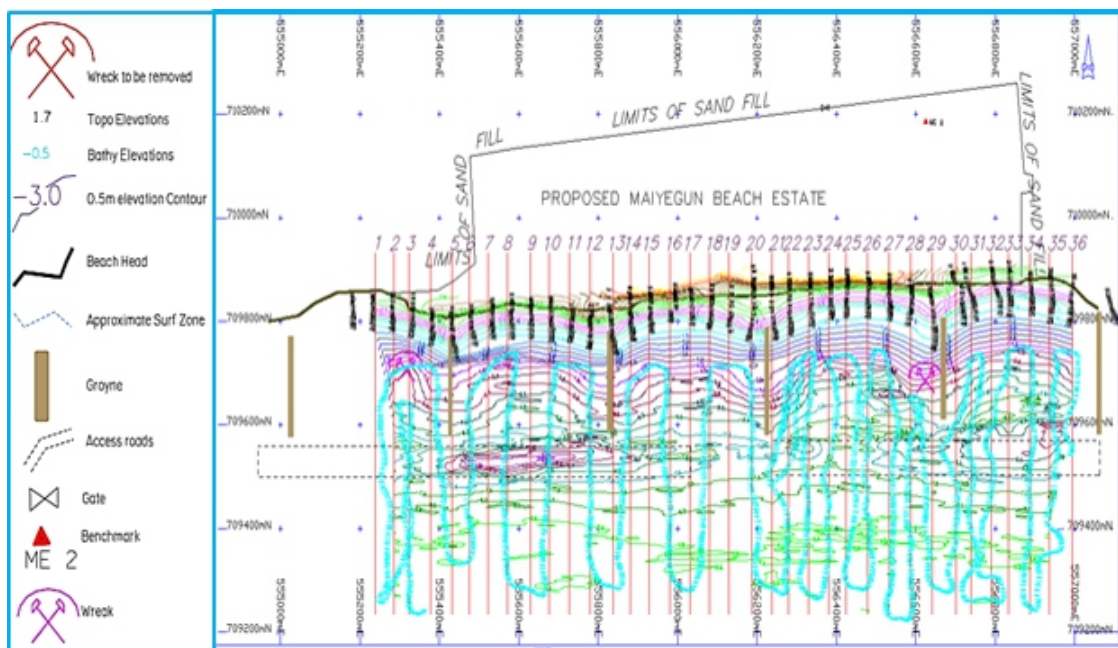


Figure 5: Preliminary data plotting process.

RESULTS

This section presents the results obtained from the analysis carried out on beach data collected from the seamless topo-bathymetric surveys.

thirty-six (36) crosslines running from the beachhead toward the sea, spaced at 50m intervals. The lines span the areas from groyne 8 (Bay 1) to groyne 12 (Bay 5). The crosslines extend up to 696.20 m from the beachhead to the sea.

Production of 3D Surface Map

The production of the profile map involved using

3D Topo-Bathy Surface Map of the Surf Zone

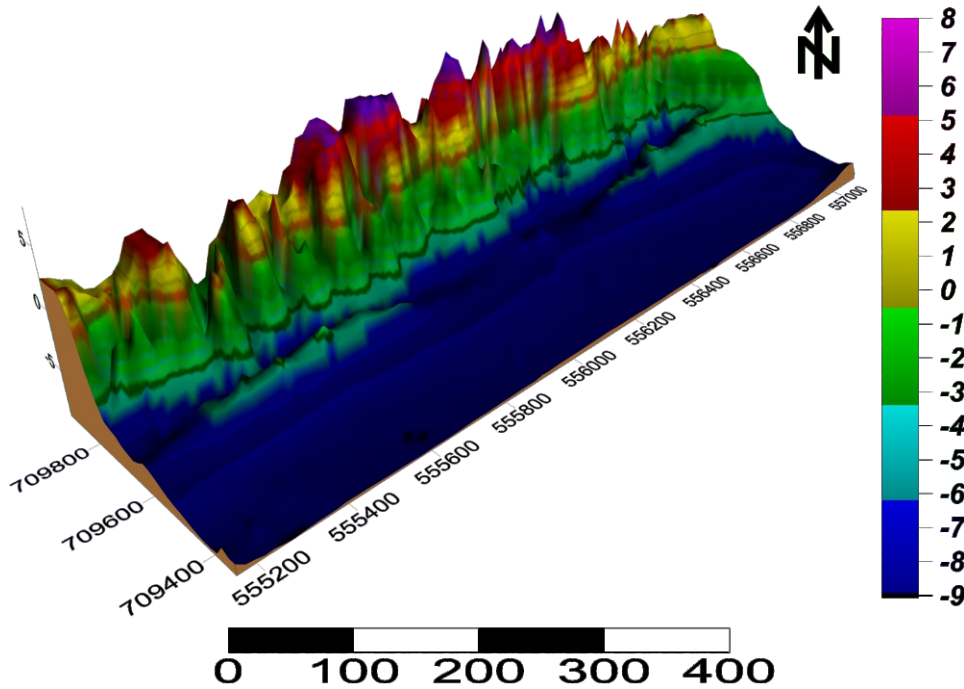


Figure 6: The produced topo-bathymetric map of the surf zone.

Figure 6 is a 3D surface map produced in Surfer 13 software. From the colour scale bar, the maximum height from the site reference BM (ME2) is 8 m, while the highest depth sounded was -9 m at a spacing of 1 m apart.

Production of Tidal and Water Level Charts

Figure 7 shows the tidal observations and water level variation tracked throughout the profile survey, which are essential to the bathymetric

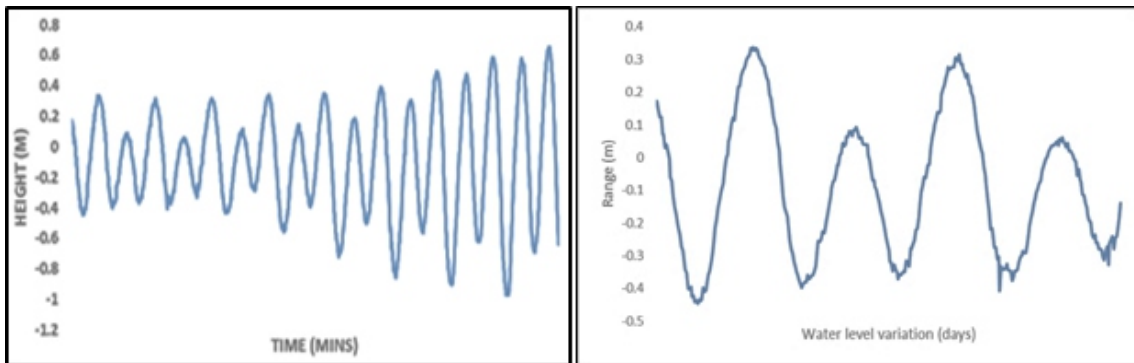


Figure 7: Tidal chart (left) water level chart (right).

From Figure 7, the observations started at neap tides and closed 10 days later at spring tides. This is reflected in the chart, with the lower tidal ranges recorded at the beginning, then transiting to much bigger ranges towards the close of the observations.

Production of Profile map

On the profile map created in Figure 8, the shaded relief map is also merged to show the area that has been impacted by the dune at the front of the groyne's heads.

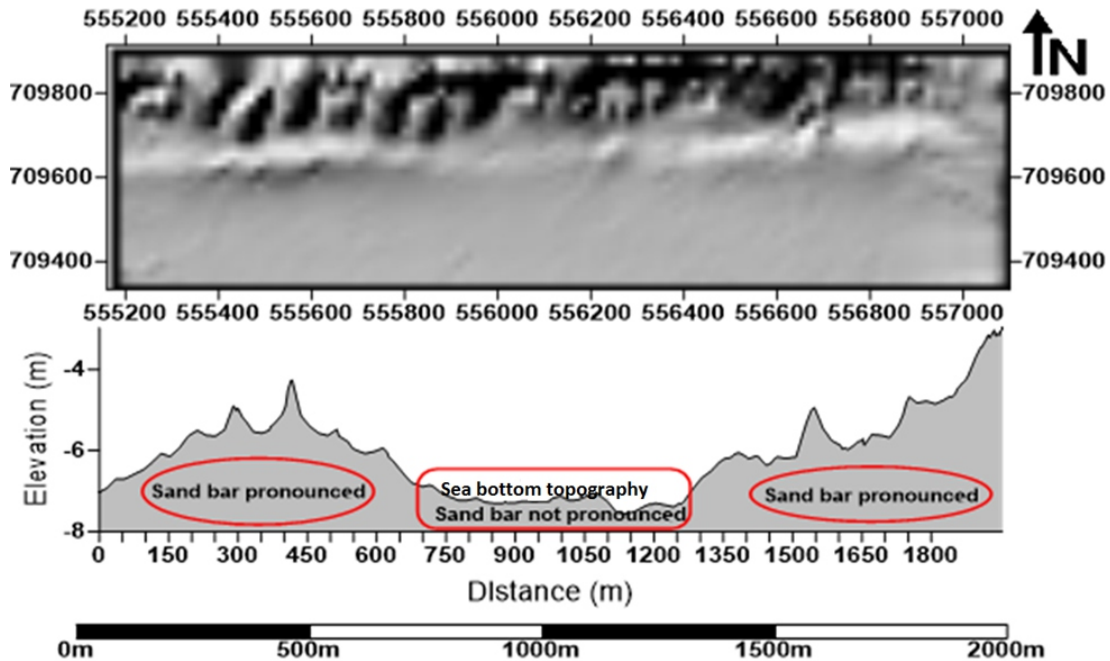


Figure 8: Profile map of covered transect lines.

Figure 8 shows the profile map produced from the topo-bathymetric datasets. The profile map's central region at distances between 700 and 1300 meters reveals that the presence of the sand bar was not particularly noticeable at elevations between -7 and -8 meters. However, the sand bars are clearly visible at elevations between -4 and -7 meters. The location of the sea bed topography is between 750 and 1300 meters, indicating some degree of irregularity in the depth configuration.

DISCUSSION

The map in Figure 6 was produced by the application of inverse distance weighting (IDW) interpolation. The interpolation assisted in overcoming the challenges posed by inaccessibility as in cases where wrecks were discovered thereby making the topographic and bathymetric surveys overlap seamlessly at unsampled few locations and the subsequent production of the 3-dimensional map of the surf zone. This type of 3D map is useful for showcasing the progression from land to water as

they interact at the shoreline borderline, and it is able to communicate to the hydrographer the transition phase at the land-water interface overlap (USGS, 2017).

From Figure 7, the tidal observation and water level monitoring results show that the tide range recorded at the commencement of observations was -0.4 m, as observation progressed toward the spring period, the range gradually increased to -1.1 m on the closing day. According to Usoro (2010), the mean spring tide range increases from 1.0 m in Lagos to 2.0 m and 3.0 m in the eastern states of Imo and Calabar, respectively. The water level fluctuated between a maximum amplitude of -0.45 m at the start of the observation and a minimum of -0.35 m near the end.

The profile map in Figure 8 reveals that the influence of the groyne is more pronounced on the left side of the map, where groyne 8 (bay 1) is located, and on the right side of the map, where groyne 12 (bay 5) is located. However, the

influence of the sand dune was less pronounced in the middle of the profile map, where groynes 9, 10, and 11 (bays 2, 3, and 4) are located. Previous studies (Vriend and Koningsveld, 2012, Neshaei and Biria, 2013, Van der Spek *et al.*, 2020) supported the possibility of sand dunes growing at the sea bed toward Groyne's head. As a result, a red buoy should be installed at these locations to warn sailors to be more cautious or, more likely, to take an alternate route to avoid a vessel mishap.

CONCLUSION

A micro section of the Nigerian coast's 3D surface and profile maps, along with information on the study site's near-shore bottom topography, have been produced by this work. The impact of the groynes constructed along the coastline also revealed the locations where the dunes along transect lines appear to be more pronounced than the others. The following recommendations were made based on the results obtained: The location of the four wrecks warrants immediate attention. Near-shore profile surveys along Nigeria's coast should be taken seriously to aid smooth navigation and coastal erosion mitigation. Observations should be taken on a monthly or yearly basis for an adequate description of the spatiotemporal changes in shore morphology. The result obtained can also be useful for validating satellite-derived bathymetry as another option to investigate its capability and as a recommendation for future research at the same location.

ACKNOWLEDGEMENT

The authors are grateful to ProEzit Geoworks and Engineering Company Ltd. No. 9 Egbelu-Mininta road, Ozuoba East-West Road, Port Harcourt for providing the data and other supports.

REFERENCES

- Anders, F.J. and Byrnes, M.R. 1991. Accuracy of shoreline change rates as determined from maps and aerial photographs. *Shore and Beach*, 59(1): 17–26.
- Badejo, O.T. and Akintoye, S.O. 2017. High and Low Water Prediction at Lagos Harbour, Nigeria. *Nigerian Journal of Technology* 36(3), 944–952. doi: 10.4314/njt.v36i3.39
- Badejo O.T. Olaleye J.B., Alademomi A.S. 2014. Tidal Characteristics and Sounding Datum Variation in Lagos State *International Journal of Innovative Research & Studies*, 3(7). 435–457.
- Cheng, J., Wang, P. and Guo, Q. 2016. Measuring Beach Profiles along a Low-Wave Energy Micro tidal Coast, West-Central Florida, USA. *Geosciences*, 6(4), 44. doi: 10.3390/geosciences 6040044
- Croituru, L., Miranda, J.J., Khattabi, A. and Lee, J.J., 2020. The Cost of Coastal Zone Degradation in Nigeria: Cross River, Delta and Lagos States. World Bank, Washington, DC. © World Bank. <https://openknowledge.worldbank.org/handle/10986/34758> License: CC BY 3.0 IGO.
- Crowell, M., Leatherman, S.P. and Buckley, M.K. 1991. Historical Shoreline Change: Error Analysis and Mapping Accuracy. *Journal of Coastal Research*, 7(3), 839–852. <http://www.jstor.org/stable/4297899>
- Emery, K.O. 1961. A simple method of measuring beach profiles. *Limnology and Oceanography*, 6, 90–93. doi: 10.4319/lo.1961.6.1.0090
- Freeman, C.W., Bernstein, D.J. and Mitasova, H. 2004. Rapid Response 3D Survey Techniques for Seamless Topo/Bathy Modeling: 2003 Hatteras Breach, North Carolina. *Shore and Beach*, 72(2), 3–7.
- Gable, C.G. and Wanetick, J.R. 1984. Survey Techniques Used To Measure Nearshore Profiles. *Coastal Engineering Proceedings*, 1(19), 126. doi: 10.9753/icce.v19.126
- Genchi, S.A., Vitale, A.J., Perillo, G.M.E., Seitz, C. and Delrieux, C.A. 2020. Mapping Topobathymetry in a Shallow Tidal Environment Using Low-Cost Technology. *Remote Sensing*, 12(9), 1394. doi: 10.3390/rs12091394
- Ibrahim, P.O., Sternberg, H., Samaila-Ija H.A., Adgidzi D. and Nwadiolor, I.J. 2022. Modelling topo-bathymetric surface using a triangulation irregular network (TIN) of Tunga Dam in Nigeria. *Applied Geomatics*. doi: 10.1007/s12518-022-00438-y

- International Hydrographic Organization IHO, 2020. Standards for Hydrographic Surveys 6th Edition IHO Publication No. 44. Available at <https://iho.int>. Assessed 2nd January, 2022.
- Kaliraj, S., Chandrasekar, N. and Magesh, N.S. 2014. Impacts of wave energy and littoral currents on shoreline erosion/accretion along the south-west coast of Kanyakumari, Tamil Nadu using DSAS and geospatial technology. *Environ. Earth Sci.*, 71, 4523–4542.
doi: 10.1007/s12665-013-2845-6
- Kankara, R.S., Selvan, S.C, Markose, V.J., Rajan, B. and Arockiaraj, S. 2015. Estimation of Long and Short Term Shoreline Changes along Andhra Pradesh Coast Using Remote Sensing and GIS Techniques. *Procedia Engineering*, 116, 855–862.
doi: 10.1016/j.proeng.2015.08.374
- Kannan, R., Anand, K.V., Sundar, V., Sannasiraj, S.A. and Rangarao, V. 2013. Shoreline changes along the Northern coast of Chennai port, from field measurements, *ISH Journal of Hydraulic Engineering*, 20(1), 24–31.
doi: 10.1080/09715010.2013.821789
- Kim, H., Hall, K., Jin J-Y, Park, G-S. and Lee, J. 2014. Empirical estimation of beach-face slope and its use for warning of berm erosion. *Journal of Measurements in Engineering*, 2, 29–42.
- Kraus, N.C. 2005. Beach Profile. In: Schwartz M. L. (eds) *Encyclopedia of Coastal Science*, 169–172. *Encyclopedia of Earth Science Series*. Springer, Dordrecht.
doi: 10.1007/1-4020-3880-1_37
- Lewicka, O., Specht, M., Stateczny, A., Specht, C., Brčić, D., Jugović, A., Widźgowski, S. and Wiśniewska, M. 2021. Analysis of GNSS, Hydroacoustic and Optoelectronic Data Integration Methods Used in Hydrography. *Sensors*, 21(23), 7831.
doi: 10.3390/s21237831
- Neshaei, M.A.L. and Biria, H.A. 2013. Impact of Groyne Construction on Beach; Case Study Anzali & Astara Coasts. 7th National Congress on Civil Engineering, 7-8 May University of Sistan and Baluchestan, Zahedan, Iran.
- Oladosu, S.O., Ehigiator-Irughe, R. and Aigbe, J.E. 2022. Seamless Topo-Bathymetric Surveys of Maiyegun Estate Waterfront Lagos State, Nigeria. *Nigerian Journal of Technology*, 41(2), 377–384.
- USGS, 2017. Advances in Topobathymetric Mapping. Retrieved February 29th, 2022 from <https://www.usgs.gov/programs/cmhrp/news/advances-topobathymetric-mapping>
- Van der Spek, B-J., Bijl, E., van de Sande, B., Poortman, S., Heijboer, D., and Bliet, B. 2020. Sandbar Breakwater: An Innovative Nature-Based Port Solution. *Water*, 12(5), 1446.
doi: 10.3390/w12051446
- Usoro, E. 2010. Nigeria. In: Bird, E.C.F. (eds) *Encyclopedia of the World's Coastal Landforms*. Springer, Dordrecht.
doi.org/10.1007/978-1-4020-8639-7_171
- Vriend D. and Koningsveld V., 2012. Design and realization of a Sandbar Breakwater, Lekki, Nigeria. Building with nature. Ecoshape Building with nature. Retrived July 10, 2022 from <https://journals.tdl.org/icce/index.php/icce/article/download/10136/9422/>
- Wu, Y. and Hung, M. 2016. Comparison of Spatial Interpolation Techniques Using Visualization and Quantitative Assessment. In (Ed.), *Applications of Spatial Statistics*. IntechOpen.
doi: 10.5772/65996
- Zabbey, N., Giadom, F.D. and Babatunde, B.B. 2019. Nigerian Coastal Environments. In *World Seas: an Environmental Evaluation (Second Edition)*, Editor: Charles Sheppard, Academic Press, 2019, 835–854.
doi: 10.1016/B978-0-12-805068-2.00042-5